Received: 11 December 2018 | Revised: 24 April 2020 | Accepted: 14 May 2020

DOI: 10.1002/dac.4497

RESEARCH ARTICLE

WILEY

Performance analysis of *M*-APSK generalised spatial modulation with constellation reassignment

Ahmad Khalid[1] | **Tahmid Quazi**[2] | **Hongjun Xu**[2] | **Sulaiman Saleem Patel**[3]

[1]Product development, Atura, Cape Town, South Africa

[2]School of Engineering, University of Kwa-Zulu Natal, Durban, South Africa

[3]Emerging Technology, Digital Consulting, KPMG Services (Pty.) Ltd., Durban, South Africa

Correspondence
Ahmad Khalid, Product development, Atura, Cape Town, South Africa.
Email: ahmadbk99@gmail.com

Summary

Generalised spatial modulation (GSM) is a recently developed multiple-input multiple-output (MIMO) technique aimed at improving data rates over conventional spatial modulation (SM) systems. However, for identical antenna array size and configurations (AASC), the bit error rate (BER) of GSM systems in comparison with SM systems is degraded. Recently, a GSM system with constellation reassignment (GSM-CR) was proposed in order to improve the BER of traditional GSM systems. However, this study focused on *M*-ary quadrature amplitude modulation (*M*-QAM) schemes. The focus of this paper is the application of a circular constellations scheme, in particular, amplitude phase shift keying (APSK) modulation, to GSM and GSM-CR systems. An analytical bound for the average BER of the proposed *M*-APSK GSM and *M*-APSK GSM-CR systems over fading channels is derived. The accuracy of this bound is verified using Monte Carlo simulation results. A 4×4 16-APSK GSM-CR system achieves a gain of 2.5 dB at BER of 10^{-5} over the traditional 16-APSK GSM system with similar AASC. Similarly, a 6×4 32-APSK GSM-CR system achieves a gain of 2 dB at BER of 10^{-5} over equivalent 32-APSK GSM system.

KEYWORDS

amplitude phase shift keying, constellation reassignment, generalised spatial modulation, genetic algorithms, MIMO communication, Rayleigh fading

1 | INTRODUCTION

1.1 | Context of research

Improving data rates and link reliability are key considerations for developing the next generation of wireless communication systems. These objectives led to the introduction of multiple-input multiple-output (MIMO) systems as an improvement to single antenna systems.[1] MIMO systems can be broken down into two broad categories. The first category focuses on multiplexing. An example of such a system is Vertical Bell Labs layered space-time (V-BLAST),[2] which attained high data rates by simultaneously transmitting independent information sequences. The spectral efficiency of such systems increased linearly with the number of transmit antennas being employed. The second category of MIMO systems focuses on achieving diversity. Alamouti was one of the first authors to introduce the MIMO space-time block coding (STBC) scheme, which attained transmit diversity.[3] Although the overall link reliability was improved, the transmission rate remained the same as that achieved by single-input single-output (SISO) systems.

In order to improve the transmission rates and spectral efficiency of MIMO systems, spatial modulation (SM) was introduced as a new technique by Mesleh et al.[4] SM systems encode data in both the signal and spatial domains, in contrast to traditional techniques which are constrained to the signal domain. In the spatial domain, bits are used to indicate which of the N_t transmit antennas in the system is active during transmission. The benefits of this are twofold: (1) the spectral efficiency of the system increases by $log_2(N_t)$ bits/s/Hz and (2) the use of only a single active transmit antenna eliminates the effects of interchannel interference (ICI) and interantenna synchronisation (IAS).[5]

Architecture of SM, however, limits the number of informations bits that may be encoded in the spatial domain since it only transmits using a single antenna. To further increase the spectral efficiency of SM systems, generalised spatial modulation (GSM) was proposed by Younis et al.[5] GSM systems optimise the encoding of information in the spatial domain, by selecting more than one antenna to be active in each time slot.[5] The overall spectral efficiency in GSM is improved, by the base-two logarithm of the number of transmit antennas, compared with SM. Although the spatial domain is now optimised, the reliability of GSM in comparison with SM is degraded due to the reintroduction of ICI.

Several schemes have been developed in order to improve the reliability of traditional GSM systems.[6-11,13] These can be divided into two categories. The first category consists of closed-loop systems, which use the channel state information (CSI) obtained from the receiver to optimise the transmission process. An example of this is the system proposed by Ma et al,[6] which improves error performance by selecting the optimal signal-space constellation at the receiver according to CSI. The second category consists of open loop systems which do not utilise feedback.[9,10,13,14] An example of such systems is the space-time block coded generalised spatial modulation (STBC-GSM) proposed by Basar et al.[9] In this scheme, the Alamouti structure was incorporated to improve the error performance over traditional GSM systems. More recently, labelling diversity (LD) has been applied to GSM systems as a means to improve their error performance. LD improves error performance by mapping the same information codewords using two bit-to-symbol mappers.[14-16] GSM with constellation reassignment (GSM-CR)[13] and GSM with STBC modulation and LD (STBC-GSM-LD)[11] are examples of recent works that have applied LD to GSM systems. It is important to note that the CR technique utilised by Naidoo et al[13] only considers a single time slot, while STBC-GSM-LD[14] transmits information bits over two time slots. The utilisation of a single time slot results in lower latency and reduced detection complexity, at the expense of reduced error performance. This study, however, only discussed quadrature amplitude modulation (QAM) schemes. The focus of this paper is to implement GSM-CR with circular constellations, in particular, amplitude phase shift keying (APSK) modulation. One of the key advantages of circular constellations is that it leads to a lower peak-to-average power ratio (PAPR), when compared with square or rectangular modulation schemes such as *M*-QAM, where *M* is the modulation order. This is achieved as a result of the reduced number of amplitude levels in *M*-APSK constellations when compared with *M*-QAM with the same modulation order.[17] This property significantly reduces the design complexity of high-power amplifiers utilised in long-range wireless communication systems. This is highlighted by the fact that APSK is the modulation scheme adopted for the latest digital video broadcasting (DVB-S2) standard, which provides the framework to improve transmission over non-linear satellite channels.[18] Therefore, emphasising the practicality and relevance of applying *M*-APSK constellations to GSM and GSM-CR for potential use in long-range wireless communication systems.

Recently, a differential SM (DSM) system for APSK modulation schemes was proposed by Martin et al[19] to improve error performance over DSM for PSK systems. To further improve the link reliability of SM systems, an optimal multiring APSK based noncoherent SM (NCSM) system assuming no CSI was proposed by Zhou et al.[20] In their letter, Zhou et al designed APSK constellations based on the theoretical symbol error probability (SER) of the NCSM system. In related work, a novel nonequiprobable APSK (NE-APSK) constellation labelling for bit-interleaved coded modulation (BICM) systems was proposed.[21] The authors herein derive the NE-APSK design from Gray-APSK by reducing the number of points in the inner ring. Similarly, Yan et al[22] optimises the parameters of Gray-APSK constellations for BICM systems using genetic algorithms (GAs). This is done by maximising the channel capacity of the system. The resultant constellations in these works[19-22] however have some limitations that leave them unsuitable for the *M*-APSK GSM and GSM-CR systems proposed in this paper: (a) they are specifically designed for coded systems, and (b) they deviate from the those recommended by the DVB-S2 standard.

The challenge of developing an *M*-APSK GSM-CR system is the design of a secondary mapper for a given *M*-APSK mapper. The objective of the design is to ensure that adjacent symbols are spaced further apart in the secondary mapper than the primary mapper. There are two approaches that are generally considered in order to design a secondary mapper. The first approach is to use geometric heuristics, but to the best of the authors' knowledge, heuristics for generalised APSK constellations have yet to be introduced. The second approach is to search over all possible constellation assignments and select the one that maximises the minimum Euclidean distance over all possible pairs of transmitted

symbols.[16] This approach commonly referred to as an exhaustive search is highly complex and impractical, since it requires the system to consider $M!$ solutions, where $(\cdot)!$ denotes the factorial function. In order to reduce the search space, Samra et al[15] presented a bounded search. Even after reducing the search space, Samra et al[15] reports that the algorithm is still too complex for constellations where $M>16$. Most recently, a new approach to mapper design based on GAs was proposed by Patel et al.[23,24] This algorithm allows for the design of mappers of higher modulation schemes, with feasible computational complexity. Thus, this algorithm is applied in this paper to design the secondary mappers for the proposed M-APSK GSM-CR system.

1.2 | Contributions

The principle contributions of this paper are summarised as follows.

1 The application of M-APSK to GSM and GSM-CR systems. The motivation for this being its lower PAPR when compared with M-QAM and its adoption in the DVB-S2 standard.
2 An analytical expressions to quantify the average bit error rate (BER) of M-APSK GSM and GSM-CR over fading channels.
3 The design of secondary mappers for the M-APSK GSM-CR system.
4 Verification of the formulated analytical expressions using Monte Carlo simulations.

1.3 | Structure and notation

The remainder of this paper is structured as follows. Section 2 details the system model for a M-APSK GSM-CR system. The theoretical BER expressions for M-APSK GSM-CR is derived in Section 4. Section 5 outlines the mapper design. Section 6 presents the theoretical and simulation BER performance of the system. Finally, Section 7 concludes the paper.

In terms of notation, this paper represents vectors and scalars in boldface and italics respectively. $\|\cdot\|_F$, $|\cdot|$ and $E\{\cdot\}$ represent the Frobenius norm of a vector, the absolute value of a complex number and statistical expectation, respectively. The $\Re(\cdot)$ represents the real component of a complex signal. Lastly, $\lfloor\cdot\rfloor$ represents the floor function of a real number.

2 | SYSTEM MODEL

The system considered in this paper is an $N_t \times N_r$ M-APSK GSM-CR system as shown in Figure 1, where N_t refers to the number of transmit antennas and N_r is the number of receive antennas. The encoder initially assigns a stream of $b = b_a + b_s$ information bits to a spatial symbol (consisting of b_a bits) and an M-APSK symbol (consisting of b_s bits). The selection of the transmit antennas refers to the spatial domain transmission while the selection of the symbol refers to the signal domain. In SM systems, the spatial domain utilises a single antenna whereas GSM systems use a pair of antennas. The spatial domain consists of all the possible pairs of transmit antennas, where the indices of these pairs

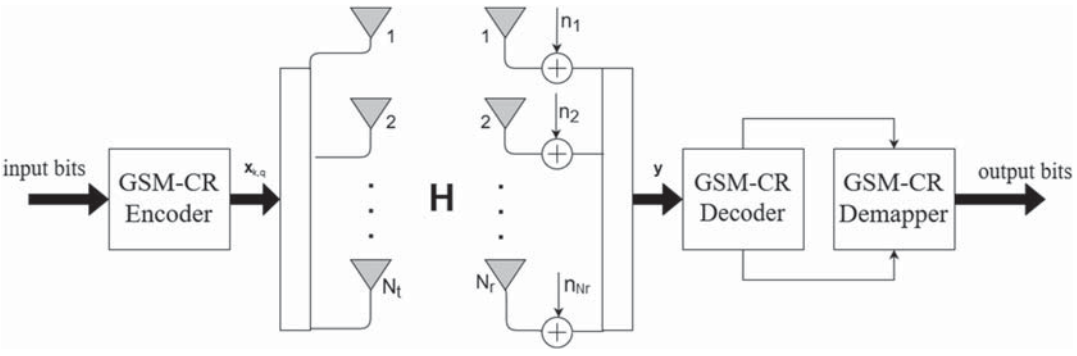

FIGURE 1 System model for GSM-CR

correspond to spatial symbols. There are $\binom{N_t}{2}$ ways to select an antenna pair from N_t transmit antennas. However, it should be noted that the number of usable antenna pair combinations must be an integer power of two. Thus, the number of antenna bits is given by $b_a = \lfloor \log_2 \binom{N_t}{2} \rfloor$. These bitsdefine codeword c_a which are indexed by k where $k \in [0 : 2^{b_a} - 1]$. This antenna pair index defines the antenna pair $\{k_1, k_2\}$ to be used during transmission. The selection of these b_a antenna pairs for an $N_t \times N_r$ GSM system is discussed by Başar et al.[9]

The signal domain in the GSM-CR system comprises two symbols mapped by $b_s = \log_2 M$ bits, where M denotes the order of the APSK modulation scheme used. These bits are mapped to an M-APSK constellation using two bit-to-symbol mappers, primary mapper ω_1 and secondary mapper ω_2. The output of these mappers are $x_q = \omega_1(q)$ and $\tilde{x}_q = \omega_2(q)$, where q represents the signal domain index and is defined by the range [0:M−1]. The output of the encoder shown in Figure 1 can be expressed as

$$\mathbf{x}_{k,q} = \left[0 \dots x_q \dots 0 \dots \tilde{x}_q \dots 0\right]^T e^{j\theta_k}, \tag{1}$$

where $\mathbf{x}_{k,q}$ is an $N_t \times 1$-dimensional transmission vector and θ_k is the rotation angle. Başar et al have presented the optimal transmit antenna pairs and the corresponding rotation angle for an $N_t \times N_r$ GSM system.[9] The same process has been applied for the proposed M-APSK GSM and M-APSK GSM-CR.

The power of the M-APSK constellation is normalised to ensure that $E\{|x_q|^2\} = E\{|\tilde{x}_q|^2\} = 1$. Modulated symbols $x_q e^{j\theta_k}$ and $\tilde{x}_q e^{j\theta_k}$ are transmitted simultaneously from antennas k_1 and k_2 over the $N_r \times N_t$ MIMO channel $\mathbf{H}$.

The received signal vector is thus given by

$$\mathbf{y} = \sqrt{\frac{\rho}{2}} \mathbf{H} \mathbf{x}_{k,q} + \mathbf{n}, \tag{2}$$

where $\mathbf{y}$ is an $N_r \times 1$-dimensional received vector subjected to $N_r \times 1$-dimensional additive white Gaussian noise (AWGN) $\mathbf{n}$. The entries of $\mathbf{H}$ and $\mathbf{n}$ are independent and identically distributed (i.i.d) according to the complex Gaussian distribution $CN(0,1)$. $\mathbf{H} = [\mathbf{h}_1 \, \mathbf{h}_2 \dots \mathbf{h}_{k_1} \dots \mathbf{h}_{k_2} \dots \mathbf{h}_{N_t}]$, where $\mathbf{h}_{k_1}$ and $\mathbf{h}_{k_2}$ are the $N_r \times 1$-dimensional vectors corresponding to transmit antenna pair index k. ρ is the average signal-to-noise ratio (SNR) at each receive antenna.

Alternatively, the received vector for the APSK GSM-CR can be represented as

$$\mathbf{y} = \sqrt{\frac{\rho}{2}} \mathbf{h}_k \mathbf{X}_q + \mathbf{n}, \tag{3}$$

where $\mathbf{X}_q = \left[x_q \, \tilde{x}_q\right]^{\mathrm{T}} e^{j\theta_k}$ is the transmitted symbol pair and $\mathbf{h}_k = [\mathbf{h}_{k_1} \mathbf{h}_{k_2}]$ is an $N_r \times 2$-dimensional channel matrix corresponding to the active antenna pair index k.

The receiver employs the ML detection rule for the estimation of transmit antenna pair index and the transmitted symbol as shown in Equation (4).

$$[\tilde{k}, \tilde{q}] = \min_{\substack{\hat{k} \in [0 : 2^{b_a} - 1] \\ \hat{q} \in [0 : M-1]}} \left\| \mathbf{y} - \sqrt{\frac{\rho}{2}} \mathbf{h}_{\hat{k}} \mathbf{X}_{\hat{q}} \right\|_F^2, \tag{4}$$

where $\tilde{k}$ and $\tilde{q}$ represent the estimated transmitted antenna pair index and M-APSK modulated index, respectively.

3 | 16-APSK AND 32-APSK CONSTELLATIONS

APSK constellations exists in multiple modulation schemes. These schemes are termed as $n_1 + n_2 + \dots + n_l$ APSK, where l is the total number of rings and n_l is the number of points on the lth ring. 4 + 12 APSK, 5 + 11 APSK, 6 + 10 APSK and 8+8 APSK are some of the common modulation schemes for 16-APSK. Among them, 4+12 APSK modulation scheme is proven to exhibit improved error performance, when considering the non-linear characteristics of a high-performance amplifier.[30-32] Similar performance has been observed in 4-12-16

APSK (32-APSK) modulation scheme.[30] Furthermore, it is also worth mentioning that 4+12 APSK and 4+12+16 APSK are the chosen modulation schemes in the latest DVB-S2 standard for satellite communications over non-linear channels.[18]

The constellation diagrams for 16-APSK and 32-APSK and the associated bit allocation for mappers ω_1 and ω_2 in decimal are shown in Figure 2. In the 16-APSK constellation, the ratio of the outer and inner radii is denoted by β_0=R_2/R_1 while the ratios in the 32-APSK constellation are defined as $\beta_1 = R_2/R_1$ and $\beta_2 = R_3/R_1$.[29]

The average symbol energy for 16-APSK is calculated as follows:

$$\begin{aligned}\bar{E}_S &= \frac{(R_1^2 + 3R_2^2)}{4} \\ &= \frac{(1 + 3\beta_0^2)R_1^2}{4}.\end{aligned} \tag{5}$$

Similarly, the average symbol energy for 32-APSK is calculated as follows:

$$\begin{aligned}\bar{E}_S &= \frac{(R_1^2 + 3R_2^2 + 4R_3^2)}{8} \\ &= \frac{(1 + 3\beta_1^2 + 4\beta_2^2)R_1^2}{8}.\end{aligned} \tag{6}$$

The peak-to-average power ratio may be calculated using the expression below[25]:

$$\text{PAPR} = 10\log\left(\frac{\max\limits_{q=0,1,\ldots,M-1}|x_q|^2}{\frac{1}{M}\sum_{q=0}^{M-1}|x_q|^2}\right)\text{dB}. \tag{7}$$

4 | BER PERFORMANCE ANALYSIS

The output of the GSM-CR detector, shown in Figure 1, estimates two quantities: the active transmit antenna pair and the transmitted symbol. As a result, the system performance depends on the error rates of these two parameters. Let P_a

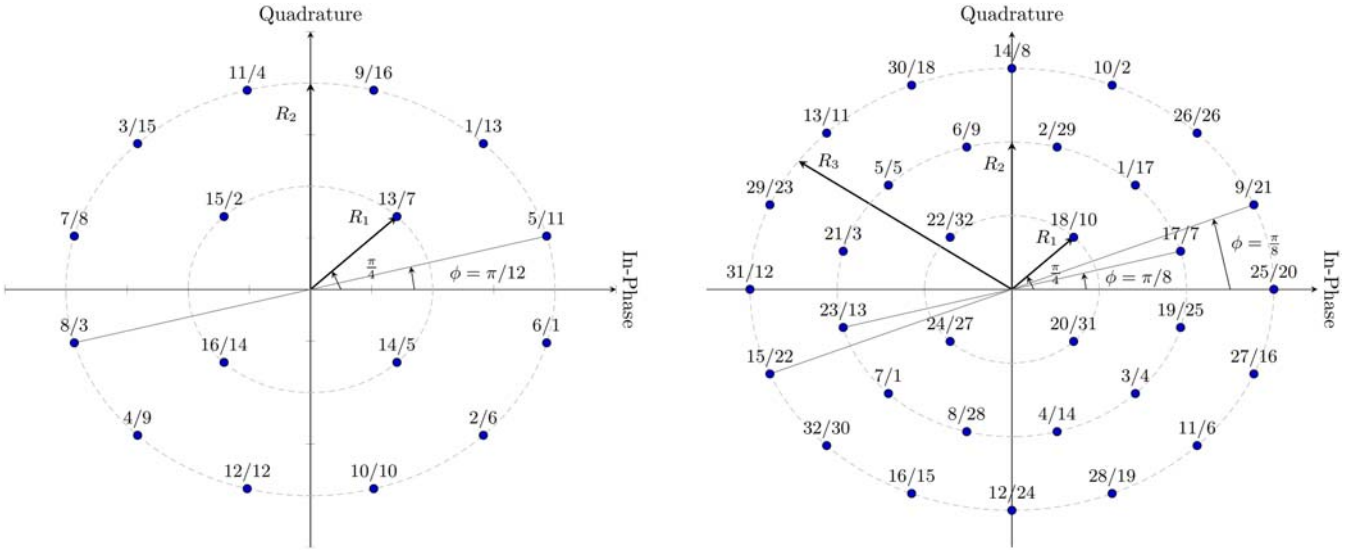

(A) Constellation Representation of 16-APSK

(B) Constellation Representation of 32-APSK

FIGURE 2 GSM-CR constellations. Key = ω_1/ω_2

denote the probability of the transmit antenna pair being incorrectly estimated, given that the modulated symbol pair is correctly detected and P_d be the probability of the modulated symbol pair being incorrectly estimated given that the transmit antenna pair is correctly detected. The overall average BER is then bounded by[4]

$$P_e \approx P_a + P_d - P_a P_d. \tag{8}$$

4.1 | Analytical BER of transmit antenna index estimation (P_a)

The average BER for the transmit antenna index is calculated by assuming the transmitted signal is correctly detected. The closed-form solution is given by Naidoo et al[13] as

$$P_a \leq \sum_{k=0}^{c-1}\sum_{q=0}^{M-1}\sum_{\substack{\hat{k}=0 \\ \hat{k}\neq k}}^{c-1} \frac{N(k,\hat{k})\mu_\alpha^{N_R}\sum_{w=0}^{N_R-1}\binom{N_R-1+w}{w}[1-\mu_\alpha]^{N_R}}{cM}, \tag{9}$$

where $N(k,\hat{k})$ is the number of bits in error between antenna pair indices k and $\hat{k}$, $\mu_\alpha = \frac{1}{2}\left(1-\sqrt{\frac{\sigma_\alpha^2}{1+\sigma_\alpha^2}}\right)$, $\sigma_\alpha^2 = (\rho/8)|x_q|^2$ where x_q is defined in Section 2 and $c = 2^{b_a}$.

4.2 | Analytical BER of symbol pair estimation (P_d)

The average BER of symbol estimation is derived using the union bound technique.[27] Assuming that the transmit antenna pair is correctly detected, the average BER for symbol pair estimation is bounded by[13]

$$P_d \leq \sum_{q=0}^{M-1}\sum_{\substack{\hat{q}=0 \\ \hat{q}\neq q}}^{M-1} \frac{N(q,\hat{q})P(\mathbf{x}_{k,q}\rightarrow\mathbf{x}_{k,\hat{q}})}{mM}, \tag{10}$$

where $m = \log_2 M$, $N(q,\hat{q})$ is the number of bit errors between symbol pair indices q and $\hat{q}$. $P(\mathbf{x}_{k,q}\rightarrow\mathbf{x}_{k,\hat{q}})$ denotes the pairwise error probability (PEP) of detecting $\mathbf{x}_{k,\hat{q}}$ given that $\mathbf{x}_{k,q}$ was transmitted.

The PEP conditioned on $\mathbf{H}$ may be expressed as

$$P\left(\mathbf{x}_{k,q}\rightarrow\mathbf{x}_{k,\hat{q}}(\mathbf{H})\right) = P\left(\left\|\mathbf{y}-\sqrt{\frac{\rho}{2}}\mathbf{H}\mathbf{x}_{k,\hat{q}}\right\|_F^2 < \left\|\mathbf{y}-\sqrt{\frac{\rho}{2}}\mathbf{H}\mathbf{x}_{k,q}\right\|_F^2\right) = \mathcal{Q}\left(\sqrt{\sum_{i=1}^{N_r} v_i}\right) \tag{11}$$

where $v_i = \frac{|u_i|^2}{2}$ and u_i is the ith element of vector $\mathbf{u}$. $\mathbf{u} = \sqrt{\frac{\rho}{2}}[\mathbf{h}_{k_1}d_1 + \mathbf{h}_{k_2}d_2]e^{j\theta_k}$, where $d_1 = \left(x_q - x_{\hat{q}}\right)$ and $d_2 = \left(\tilde{x}_q - \tilde{x}_{\hat{q}}\right)$. The derivation of the Q-function can be found in Appendix A1.

In order to evaluate Equation (11), the trapezoidal rule[34] for numerical integration is applied to the $\mathcal{Q}$-function, which leads to

$$\mathcal{Q}\left(\sqrt{x}\right) = \frac{1}{4n}\exp\left(-\frac{x}{2}\right) + \frac{1}{2n}\sum_{c=1}^{n-1}\exp\left(-\frac{x}{S_c}\right), \tag{12}$$

where $S_c = 2\sin^2\left(\frac{c\pi}{2n}\right)$ and n is the number of summations. It is shown by Quazi[34] that choosing n greater than six results in sufficient accuracy in the numerical integration.

Using Equation (12), Equation (11) can be simplified to

$$P\left(\mathbf{x}_{k,q} \to \mathbf{x}_{k,\hat{q}}(\mathbf{H})\right) = \mathcal{Q}\left(\sqrt{\sum_{i=1}^{N_r} v_i}\right)$$
$$= \frac{1}{4n}\exp\left(-\frac{\sum_{i=1}^{N_r} v_i}{2}\right) + \frac{1}{2n}\sum_{c=1}^{n-1}\exp\left(-\frac{\sum_{i=1}^{N_r} v_i}{S_c}\right) \tag{13}$$
$$= \frac{1}{4n}\prod_{i=1}^{N_r}\left(\exp\left(-\frac{v_i}{2}\right)\right) + \frac{1}{2n}\sum_{c=1}^{n-1}\prod_{i=1}^{N_r}\left(\exp\left(-\frac{v_i}{S_c}\right)\right).$$

The PEP conditioned on **H** defined in Equation (13) is averaged by integrating over the fading distribution,

$$P\left(\mathbf{x}_{k,q} \to \mathbf{x}_{k,\hat{q}}\right) = \int_0^\infty \mathcal{Q}\left(\sqrt{\sum_{i=1}^{N_r} v_i}\right) P(v_i)dv_i, \tag{14}$$

where the Gaussian function, $Q(x)$, is defined above and the fading probability density function (PDF) of v_i is given by[26]

$$P(v_i) = \frac{1}{\bar{v}_i}\exp\left(-\frac{v_i}{\bar{v}_i}\right), \tag{15}$$

where the variance $\bar{v}_i$ is given by

$$\bar{v}_i = E\left\{\frac{1}{2}|u_i|^2\right\} = E\left\{\frac{1}{2}\left|\sqrt{\frac{\rho}{2}}[h_{i,k_1}d_1 + h_{i,k,2}d_2]e^{j\theta_k}\right|^2\right\} = \frac{\rho}{4}\left(|d_1|^2 + |d_2|^2\right), \tag{16}$$

where the reader is reminded that $h_{i,k_1}, h_{i,k_2} \sim CN(0,1)$ as defined in Section 2. Since the result in Equation (16) show that $\bar{v}_i$ is independent of i, $\bar{v} = \bar{v}_i$ for all $i \in [1{:}N_r]$.

Substituting Equation (13) in Equation (14), the unconditional probability can be written as

$$P\left(\mathbf{x}_{k,q} \to \mathbf{x}_{k,\hat{q}}\right) = \int_0^\infty \frac{1}{4n}\prod_{i=1}^{N_r}\left(\exp\left(-\frac{v_i}{2}\right)\right) + \frac{1}{2n}\sum_{c=1}^{n-1}\prod_{i=1}^{N_r}\left(\exp\left(-\frac{v_i}{S_c}\right)\right)P(v_i)dv_i$$
$$= \frac{1}{4n}\prod_{i=1}^{N_r}\left(\mathcal{M}\left(\frac{1}{2}\right)\right) + \frac{1}{2n}\sum_{c=1}^{n-1}\prod_{i=1}^{N_r}\left(\mathcal{M}\left(\frac{1}{S_c}\right)\right), \tag{17}$$

where $\mathcal{M}(\cdot)$ is the moment generating function (MGF) for Rayleigh Fading and is defined by[28]

$$\mathcal{M}(s) = (1 + s\bar{v})^{-1}. \tag{18}$$

Since, the MGF is independent of i as shown in Equation (18), $\prod_{i=1}^{N_r}\mathcal{M}(s) = [\mathcal{M}(s)]^{N_r}$. Hence, the average BER expression of symbol estimation may be obtained by substituting the unconditioned probability derived in Equation (17) in overall bound defined in Equation (10). The resultant final expression for P_d is as follows:

$$P_d \le \frac{1}{mM}\sum_{q=0}^{M-1}\sum_{\substack{\hat{q}=0 \\ \hat{q}\neq q}}^{M-1} N(q,\hat{q})\frac{1}{4n}\left(1 + \frac{\bar{v}}{2}\right)^{-N_r} + \frac{1}{2n}\sum_{c=1}^{n-1}\left(1 + \frac{\bar{v}}{S_c}\right)^{-N_r}. \tag{19}$$

5 | CONSTELLATION REASSIGNMENT MAPPER DESIGN

In order to achieve LD, CR requires the use of primary and secondary mappers. For the M-APSK GSM-CR system, primary mapper (ω_1) is designed to follow a Gray-coded structure, which is proven to be optimal as discussed by Samra

et al.[15] As discussed in Section 1, there is no precedence for the design of secondary mappers (ω_2) for the M-APSK constellations considered in this paper. Thus, the generic approach proposed by Patel et al[23] for LD systems is adopted in this paper. This approach utilises a GA to design secondary mappers for space-time labelling diversity (STLD) systems. Since both STLD and CR systems require a secondary mapper to achieve LD, this algorithm is adapted and applied for the M-APSK GSM-CR system.

The analytical expressions derived in Section 4 for the error performance of M-APSK GSM-CR system are used to guide the mapper design process. In particular, since CR only affects the probability of a symbol pair estimation error (P_d), the results of Section 4.2 form the framework for this design. The first stage of this design is similar to that employed by Xu et al,[14] which considers a high SNR approximation of the symbol pair estimation, P_d. At high SNR, the Rayleigh fading MGF (defined in Equation 18) is dominated by its second term. As such, following on from Equation (19), P_d at high SNR is approximated as

$$P_d^{\text{high SNR}} \leq \frac{1}{mM}\sum_{q=0}^{M-1}\sum_{\hat{q}=0}^{M-1} N(q,\hat{q})\frac{1}{4n}\left(\frac{\rho}{8}\left(|d_1|^2+|d_2|^2\right)\right)^{-N_r} + \frac{1}{2n}\sum_{i=1}^{n-1}\left(\frac{\rho}{4S_i}\left(|d_1|^2+|d_1|^2\right)\right)^{-N_r}, \tag{20}$$

where Equation (16) has been substituted into the expression. It is thus apparent that the performance of the system is dependent on the sum of the squared distances, given by

$$\mathcal{D} = |d_1|^2 + |d_2|^2 = |x_q - x_{\hat{q}}|^2 + |\tilde{x}_q - \tilde{x}_{\hat{q}}|^2. \tag{21}$$

Higher values of $\mathcal{D}$ result in lower probability P_d. Thus, the error floor of P_d is set by the minimum value of $\mathcal{D}$, which is denoted as $\mathcal{D}_{\min}$. It then follows that the overall objective of mapper design for CR systems is to produce mapper ω_2 given ω_1 in order to maximise $\mathcal{D}_{\min}$.

5.1 | Description of GA

The GA described by Patel et al[23] considers the case where ω_1 is known and ω_2 is desired. The output of this algorithm is obtained from an iterative heuristic search through the candidate mapper space.

The block diagram in Figure 3 provides a high-level illustration of the GA designed by Patel et al.[23] Candidate secondary mappers are encoded into data structures called 'chromosomes', which consist of subunits referred to as 'genes'. The set of chromosomes considered at each iteration of the algorithm is referred to as the 'population'. The notation used in this section is to represent genes, chromosomes and the population with variables ε, $\mathcal{E}$ and ϱ, respectively.

In the remainder of this section, the authors provide a summarised discussion of each stage of the GA.

5.1.1 | Genetic coding

'Genetic coding' is the term used to describe the representation of each candidate mapper as a chromosome. Each chromosome consists of genes, ε_i, $i \in [1:M]$, each of which corresponds to a symbol from the M-APSK constellation. The corresponding value assigned to each gene of the chromosome is the binary value associated with that constellation point. Thus, the chromosome $\mathcal{E}$ is defined by

$$\mathcal{E} = [\varepsilon_1 \varepsilon_2 ... \varepsilon_{M-1} \varepsilon_M]. \tag{22}$$

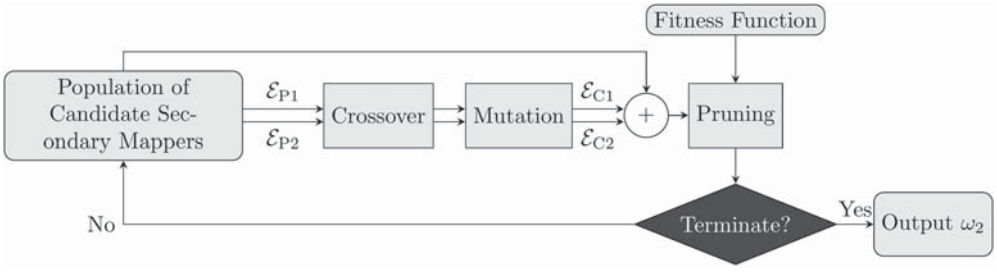

FIGURE 3 Block diagram of genetic algorithm for CR mapper design. $\mathcal{E}_{P1}, \mathcal{E}_{P2}$ = parent chromosomes. $\mathcal{E}_{C1}, \mathcal{E}_{C2}$ = child chromosomes

An illustration of the 16-APSK and 32-APSK constellations considered in this paper, explicitly showing the location of each gene, is given in Figure 4.

5.1.2 | Generating a population of chromosomes

The population of chromosomes refers to the set of candidate secondary mappers evaluated by the GA at each iteration. Hence, the population during the *nth* iteration, ϱ_{n}, is defined as

$$\varrho_n = \left\{\mathcal{E}_{1,n}\,\mathcal{E}_{2,n}\ldots\mathcal{E}_{(z-1),n}\,\mathcal{E}_{z,n}\right\}, \tag{23}$$

where z is the number of chromosomes in the population. As suggested by Patel et al,[23] the initial population (ϱ_0) consists of a set of z chromosomes selected at random from the $M!$ candidate mapper space.

5.1.3 | Crossover and mutation

The processes of crossover and mutation are the most important elements of the GA.[35] Crossover and mutation model the biological process of evolution to generate progressively more optimal population ϱ at each iteration. Hence, the population $\varrho_{\mathrm{n}+1}$ is more optimal than ϱ_{n}.

The κ-point hypersphere swap crossover (κ-HSX) proposed by Patel et al[23] for STLD mapper design is implemented for this GA. The authors note that the goal of mapper design in STLD and CR systems are similar, thus no modifications to κ-HSX are needed to apply it in the CR context. The reader is referred to the original work[23] for full details of the κ-HSX process, including a procedural example of the swapping process.

Mutation is a random event that occurs when a child chromosome undergoes further changes after crossover. The probability of a mutation occurring for a given child chromosome is denoted P_{mutation}. If a mutation occurs, two genes are randomly selected from the child chromosome and swapped. Patel et al[23] highlight that, unlike crossover, no properties from the parent chromosomes are used to inform this swap.

5.1.4 | Pruning

The purpose of pruning at end of each iteration is to discard the least-fit chromosomes from the population. This is done to model the biological process of 'natural selection'. In the GA for mapper design, $2\times\binom{z}{2}$ chromosomes are discarded at the end of each iteration. In this way, the population size at the start of each iteration remains fixed at z.

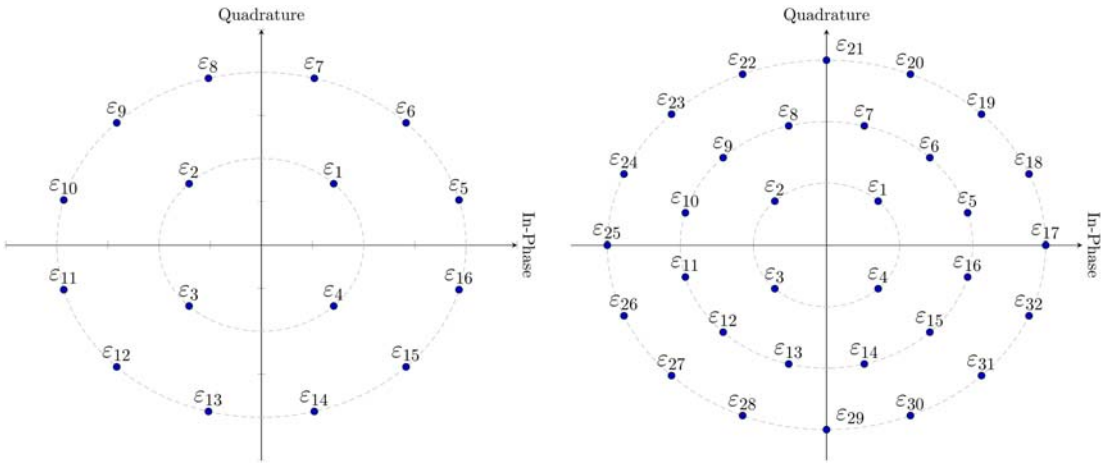

(A) 16-APSK **(B)** 32-APSK

FIGURE 4 Illustrating the position of genes in M-APSK constellations

When pruning the population, a metric to quantitatively evaluate chromosomes is necessary. As mentioned previously, the error floor of the symbol pair estimation probability of the GSM-CR system is set by the minimum summed-squared distance, $\mathcal{D}_{\min}$. This suggests that an appropriate fitness function to evaluate chromosome $\mathcal{E}$ when pruning is given by

$$\Psi(\mathcal{E}) = \min_{q,\hat{q}\in[0:M-1]} \left\{ |x_q - x_{\hat{q}}|^2 + |\omega_{\mathcal{E}}(q) - \omega_{\mathcal{E}}(\hat{q})|^2 \right\}, \tag{24}$$

where $\omega_{\mathcal{E}}$ is the mapper represented by chromosome $\mathcal{E}$. Equation (24) is obtained from Equation (21) by obtaining $\tilde{x}_q$ and $\tilde{x}_{\hat{q}}$ from $\omega_{\mathcal{E}}$. Thus, the z chromosomes with the highest fitness, evaluated using Equation (24), form the population ϱ_{n+1} at the end of the pruning stage.

The authors emphasise that the fitness function in Equation (24) is the key difference between the GA for CR systems and its original variant for STLD systems.[23]

5.1.5 | Termination

Termination of a GA occurs when the population is deemed to contain an optimal solution or if the algorithm determines that no feasible solution can be found.

As suggested by Patel et al,[23] the population is said to contain an optimal solution when all chromosomes converge to the same genotype (i.e., they all have the same fitness). All chromosomes in the population are then considered equally optimal, and any of them may be selected as the output.

Patel et al[23] also constrain the algorithm to run for a maximum of $n_{\max}$ iterations to ensure that it is computationally feasible, where $n_{\max} \ll M^5$. If the maximum number of iterations is reached, it is assumed that the GA will not converge. In this case, the fittest chromosome from the population is selected as the output.

5.1.6 | Implementation

When implementing the algorithm to produce secondary mappers for the context of CR for 16-APSK and 32-APSK constellations, the following parameters were used: $z = 8$ and $P_{\text{mutation}} = 0.1$. The κ-HSX algorithm is implemented with parameter $\kappa = \frac{M-4}{2}$. The maximum number of iterations for the GA is set to $n_{\max} = 10^4$ for 16-APSK and $n_{\max} = 10^6$ for 32-APSK constellation.

6 | RESULTS AND DISCUSSION

The section begins with a discussion of the PAPR comparison between M-APSK constellations and the more widely used M-QAM constellations. The values for M-APSK and M-QAM PAPR were obtained using Equation (7) and are shown in Table 1. It is clearly evident that the lower number of amplitude levels in APSK constellations results in a lower PAPR when compared with QAM.[12] This characteristic of APSK constellations justifies its adoption in long-range wireless communication systems. This motivates for the application of M-APSK constellations to advance SM systems such as GSM and GSM-CR in this paper. Consequently, the performance study of the proposed M-APSK GSM and M-APSK GSM-CR systems is presented in what follows.

The performance of the proposed systems is presented in terms of the average BER analytical expression developed in Section 4. These results are validated using Monte Carlo simulations for various antenna array sizes and configurations. Thereafter, performance comparisons are made between SM, GSM and GSM-CR systems with equivalent spectral efficiencies. In the performance study, assume $N_r = 4$ and that the channel remains constant for the duration of a single transmission.

Monte Carlo simulations were performed using the ML detection rule defined in Equation (4) with the following assumptions: Rayleigh flat fading channel, full knowledge of channel at the receiver, the antennas at the transmitter and receiver are separated wide enough to avoid correlation, maximal ratio combining reception is used at the receiver, and the total transmit power is split equally between the two active transmit antennas. Rotation angles and the selection of the transmit antenna pairs are based on the design proposed by Başar et al.[9] The transmit antenna pairs used for

TABLE 1 PAPR of *M*-APSK and *M*-QAM constellations

	16-APSK	16-QAM	32-APSK	32-QAM
PAPR (dB)	1.1	2.6	1.9	3.2

TABLE 2 $4 \times N_r$ antenna pairs

Antenna array sizes and configurations	$4\times N_r$			
Transmit antenna pair	(1,3)	(1,4)	(2,3)	(2,4)
Rotation angle (16-APSK)	0	$\pi/4$	$\pi/4$	0
Rotation angle (32-APSK)	0	$\pi/4$	$\pi/4$	0

TABLE 3 $6 \times N_r$ antenna pairs

Antenna array sizes and configurations	$6\times N_r$							
Transmit antenna pair	(1,2)	(3,4)	(5,6)	(2,3)	(4,5)	(1,6)	(1,3)	(2,4)
Rotation angle (16-APSK)	0	0	0	$\pi/3$	$\pi/3$	$\pi/3$	$2\pi/3$	$2\pi/3$
Rotation angle (32-APSK)	0	0	0	$\pi/6$	$\pi/6$	$\pi/6$	$\pi/3$	$\pi/3$

M-APSK GSM and *M*-APSK GSM-CR were obtained from Başar et al for a $4 \times N_r$ and $6 \times N_r$ and shown in Tables 2 and 3, respectively.[9] Since it is not possible to derive rotation angles for $M > 4$,[9] an exhaustive search via computer simulation is conducted to maximise the average BER performance. The results obtained are outlined in Tables 2 and 3. Figures 5–8 show the average BER of SM, GSM and GSM-CR with various AASC. In order to ensure a fair comparison, identical spatial mappings were employed for both GSM and GSM-CR systems. The simulation results for all cases of GSM and GSM-CR systems are observed to closely follow the union bound in high SNR region, thus verifying the analytical average BER expressions derived in Section 4. It is also evident that in all cases, the GSM-CR outperforms the GSM and SM systems. Figures 5 and 6 show the average BER for 4×4 antenna configuration for 16-APSK and 32-APSK, respectively. These correspond to spectral efficiencies of 6 and 7 bits/s/Hz, respectively. As the graphs in Figure 5 show, the 16-APSK GSM-CR system achieves the gain of 2.5 dB over its equivalent GSM system and 1.5 dB in comparison with its equivalent SM system at BER of 10^{-5}. Furthermore, GSM systems are shown to have slightly degraded performance in comparison with SM. The higher error probability of detecting two transmit antennas in GSM, in comparison with the single transmit antenna detection in SM, is the reason for the degraded performance.[5] In Figure 6, the 32-APSK GSM-CR systems achieves gains of 2.2 and 2dB at BER of 10^{-5} in comparison with its equivalent GSM and SM systems, respectively. Figures 7 and 8 show the average BER for 6×4 antenna configuration for 16-APSK and 32-APSK, respectively. These correspond to spectral efficiencies of 7 and 8 bits/s/Hz, respectively. It can be seen in Figure 7 that the 16-APSK GSM-CR system achieves the gain of 2.5 dB over its equivalent GSM system and 1.5 dB in

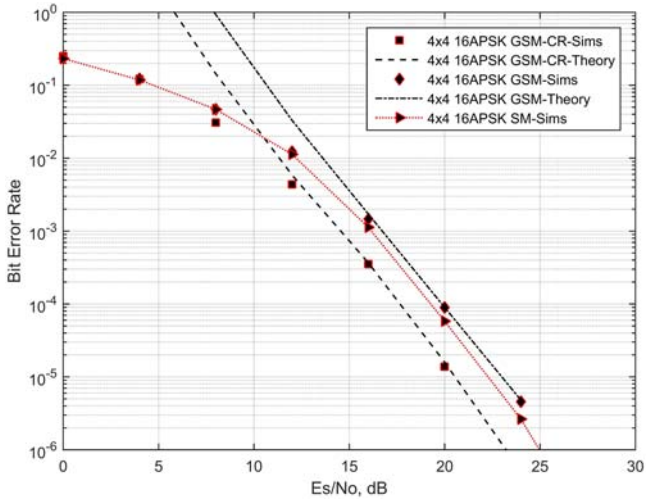

FIGURE 5 Average BER—6 bits/s/Hz configuration

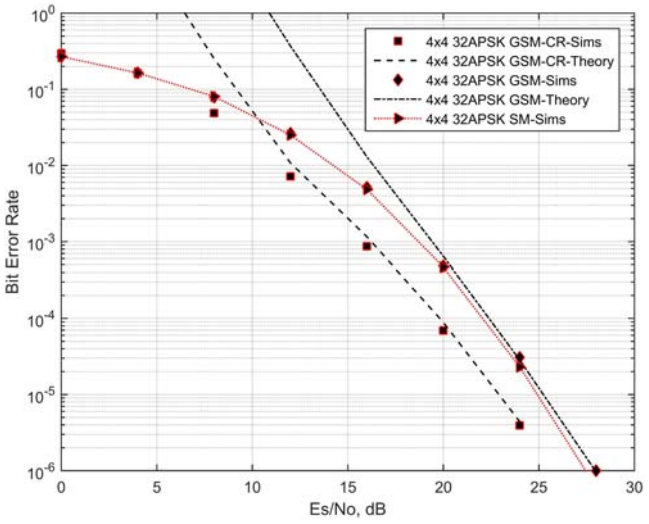

FIGURE 6 Average BER—7 bits/s/Hz configuration

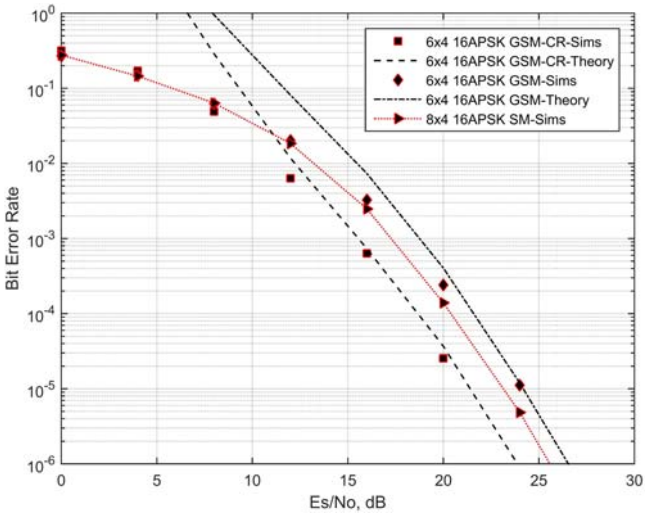

FIGURE 7 Average BER—7 bits/s/Hz configuration

comparison with its equivalent SM system at BER of 10^{-5}. In Figure 8, the 32-APSK GSM-CR systems achieves gains of 2 and 1.2 dB at BER of 10^{-5} in comparison with its equivalent GSM and SM systems, respectively. It should be noted that similar performance improvements were observed in *M*-QAM GSM-CR over SM and GSM in the original work done by Naidoo et al.[13]

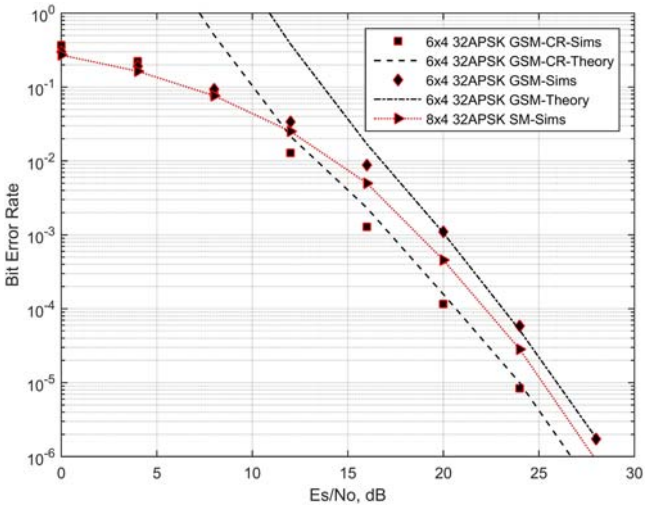

FIGURE 8 Average BER—8 bits/s/Hz configurations

The performance gains for the M-APSK GSM-CR system over the M-APSK GSM system in various AASC is attributed to the improved error performance of symbol pair estimation, P_d. This is due to the introduction of labelling diversity in the system. Since P_d has been significantly improved, using Equation (8), it can be concluded that the overall probability of the system is now bounded by P_a if P_d approaches 0. Hence, for future works, the next logical step would be to improve the average BER of transmit antenna pair estimation, P_a, in order to further improve link reliability of GSM systems.

7 | CONCLUSION

This paper presents a performance study of an M-APSK GSM-CR system. An analytical framework for the average BER is formulated for the M-APSK GSM-CR system. The framework guides the design of the GA used to develop secondary mappers for APSK. The first set of results focus on a PAPR comparison between M-APSK constellations to M-QAM. As expected, the APSK constellations achieve a lower PAPR as compared with QAM. The second set of results focus on validating the theoretical expression derived by the results of Monte Carlo simulations, which show a tight bound in the high SNR region. The results presented further show that the M-APSK GSM-CR outperforms its equivalent GSM and SM systems in various antenna array sizes and configurations. A 4×4 16-APSK GSM-CR systems achieve gains of 2.5 dB over its equivalent GSM system and 1.5 dB in comparison with its equivalent SM system at BER of 10^{-5}. Similar gains are evident for 32-APSK and at various different spectral efficiencies.

8 | FUTURE WORKS

This paper opens up the possibility of future research work to be done in multiple areas. Firstly, the error performance may be improved by application of more recent APSK constellations with the proposed GSM-CR system. The NE-APSK constellations[21] is one such constellation that may be considered for the proposed system. The generic mapper design detailed in this paper allows the system to generate secondary mappers for any type and size of constellations. Secondly, it has been shown in this paper that the overall probability of a GSM-CR system is bounded by the error probability of antenna pair estimation. The focus should therefore be to enhance P_a in order to further improve the link reliability of GSM and GSM-CR systems. Lastly, there have been more advanced SM systems that further improve performance when compared GSM-CR such as ST-QSM, GQSM and EQSM.[36-38] In future work, the authors will consider the application of circular constellations to such systems.

ORCID

Ahmad Khalid https://orcid.org/0000-0002-9261-707X
Tahmid Quazi https://orcid.org/0000-0002-1288-4224
Hongjun Xu https://orcid.org/0000-0002-5768-1965
Sulaiman Saleem Patel https://orcid.org/0000-0003-3557-3645

REFERENCES

1. Foschini GJ. Layered space-time architecture for wireless communication in a fading environment when using multi-element antennas. *Bell Labs Tech J*. 1996;1(2):41-59.
2. Wolniansky PW, Foschini GJ, Golden GD, Valenzuela RA. V-BLAST: an architecture for realizing very high data rates over the rich-scattering wireless channel. In: URSI International Symposium on Signals, Systems, and Electronics. Conference Proceedings; 1998: 295-300.
3. Alamouti SM. A simple transmit diversity technique for wireless communications. *IEEE Journal on Selected Areas in Communications*. 1998;16(8):1451-1458.
4. Mesleh RY, Haas H, Sinanovic S, Ahn CW, Yun S. Spatial modulation. *IEEE Transactions on Vehicular Technol*. 2008;57(4):2228-2241.
5. Younis A, Serafimovski N, Mesleh R, Haas H. Generalised spatial modulation. In: Conference Record of the Forty Fourth Asilomar Conference on Signals, Systems and Computers; 2010:1498-1502.
6. Ma N, Wang A, Han C, Ji Y. Adaptive joint mapping generalised spatial modulation. In: IEEE International Conference on Communications in China; 2012:520-523.
7. YiÄ§it Z, Baar E. High-rate generalized spatial modulation. *24th Signal Processing and Communication Application Conference (SIU)*. 2016:1117-1120.

8. Zhou Y, Yuan D, Zhou X, Zhang H. Trellis coded generalized spatial modulation. In: IEEE 79th Vehicular Technology Conference (VTC Spring); 2014:1-5.
9. Başar E, Aygölü, Panayrc E, Poor HV. Space-time block coding for spatial modulation. In: 21st Annual IEEE International Symposium on Personal, Indoor and Mobile Radio Communications; 2010:803-808.
10. Sundaravadivu K, Bharathi S. STBC codes for generalized spatial modulation in MIMO systems. In: IEEE International Conference ON Emerging Trends in Computing, Communication and Nanotechnology; 2013:486-490.
11. Govindasamy K, Xu H, Pillay N. Space-time block coded spatial modulation with labeling diversity. *Int J Commun Syst*. 2018;31(1):e3395.
12. Baldi M, Chiaraluce F, Angelis A, Marchesani R, Schillaci S. A comparison between APSK and QAM in wireless tactical scenarios for land mobile systems. *J Wireless Com Network*. 2012:317.
13. Naidoo N. Enhanced performance and efficiency schemes for generalised spatial modulation. Durban, South Africa: School of Eng., University of Kwa-Zulu Natal; 2017.
14. Xu H, Govindasamy K, Pillay N. Uncoded space-time labeling diversity. *IEEE Communications Letters*. 2016;20(8):1511-1514.
15. Samra H, Ding Z, Hahn PM. Symbol mapping diversity design for multiple packet transmissions. *IEEE Trans Commun*. 2005;53(5): 810-817.
16. Seddik KG, Ibrahim AS, Ray Liu KJ. Trans-modulation in wireless relay networks. *IEEE Commun Lett*. 2008;12(3):170-172.
17. Quazi T, Xu H. BER performance of a hierarchical APSK UEP system over Nakagami-m fading. *SAIEE Africa Res J*. 2016;107(4):230-236.
18. Morello A, Mignone V. DVB-S2: the second generation standard for satellite broad-band services. *Proc IEEE*. 2006;94(1):210-227.
19. Martin PA. Differential spatial modulation for APSK in time-varying fading channels. *IEEE Communications Letters*. 2015;19(7): 1261-1264.
20. Zhou Y, Zhang H, Zhang P, Yuan D. Non-coherent spatial modulation and optimal multi-ring APSK constellation design. *IEEE Commun Lett*. 2018;22(5):950-953.
21. Yang F, Yan K, Xie Q, Song J. Non-equiprobable APSK constellation labeling design for BICM systems. *IEEE Communications Letters*. 2013;17(6):1276-1279.
22. Yan K, Yang F, Pan C, Song J, Ren F, Li J. Genetic algorithm aided gray-APSK constellation optimization. In: 9th International Wireless Communications and Mobile Computing Conference; 2013:1705-1709.
23. Patel SS, Quazi T, Xu H. A genetic algorithm for designing uncoded space-time labelling diversity mappers. In: 2018 IEEE International Workshop on Signal Processing Systems; 2018:1-6.
24. Patel SS. Uncoded space-time labelling diversity: data rate and reliability enhancements and application to real-world satellite broadcasting. Durban, South Africa: School of Eng., University of Kwa-Zulu Natal; 2019.
25. Myung H, Goodman D. *Single Carrier FDMA: A New Air Interface for Long Term Evolution*. New York: John Wiley and Sons; 2008.
26. Goldsmith A. *Wireless Communications*. Cambridge, USA: Cambridge University Press; 2005.
27. Proakis JG. *Digital Communications*. 4th Edition. New York, USA: McGraw-Hill Education; 2001.
28. Simon MK, Alouini M. *Digital Communication Over Fading Channels: A Unified Approach to Performance Analysis*. New York: John Wiley and Sons; 2002.
29. Sung W, Kang S, Kim P, Chang D, Shin D. Performance analysis of APSK modulation for DVB-S2 transmission over nonlinear channels. *Int J Satellite Commun Netw*. 2009;27(6):295-311.
30. Kim J, Sin CS, Lee SU. Improved performance of APSK modulation scheme for satellite system. In: 6th International Conference on Information, Communications Signal Processing; 2007:1-4.
31. AbdulHussein H, Al-Asady, Ibnkahla M. Performance evaluation and total degradation of 16-QAM modulations over satellite channels. In: Canadian Conference on Electrical and Computer Engineering, Vol. 2; 2004:1187-1190.
32. De Gaudenzi R, Guillen i Fabregas A, Martinez A. Performance analysis of turbo-coded APSK modulations over nonlinear satellite channels. *IEEE Trans Wireless Commun*. 2006;5(9):2396-2407.
33. Craig JW. A new, simple and exact result for calculating the probability of error for two-dimensional signal constellations. In: MILCOM 91 - Conference record, Vol. 2; 1991:571-575.
34. Quazi T. Cross-layer design for the transmission of multimedia traffic over fading channels. Durban, South Africa: School of Eng., University of Kwa-Zulu Natal; 2009.
35. Ahmed ZH. An improved genetic algorithm using adaptive mutation operator for the quadratic assignment problem. In: 38th International Conference on Telecommunications and Signal Processing; 2015:1-5.
36. Yigit Z, Basar E. Space-time quadrature spatial modulation. In: IEEE International Black Sea Conference on Communications and Networking; 2017:1-5.
37. Castillo-Soria F, Cortez J, Gutierrez C, Luna-Rivera JM, Garcia-Barrientos A. Extended quadrature spatial modulation for MIMO wireless communications. *Phys Commun*. 2018;32:88-95.
38. Mesleh R, Ikki SS, Aggoune HM. Quadrature spatial modulation. *IEEE Trans Veh Technol*. 2015;64(6):2738-2742.

How to cite this article: Khalid A, Quazi T, Xu H, Patel SS. Performance analysis of *M*-APSK generalised spatial modulation with constellation reassignment. *Int J Commun Syst*. 2020;33:e4497. https://doi.org/10.1002/dac.4497

APPENDIX A: DERIVATION OF THE *Q*-FUNCTION DERIVATION

In this section, the derivation of the *Q*-function for the proposed system is shown.

Rewriting using alternative notation shown in Equation (3) yields

$$\begin{aligned} P\left(\mathbf{x}_{k,q} \to \mathbf{x}_{k,\hat{q}}(\mathbf{H})\right) &= P\left(\left\|\sqrt{\tfrac{\rho}{2}}\mathbf{h}_k\left[\mathbf{X}_q - \mathbf{X}_{\hat{q}}\right] + \mathbf{n}\right\|_F^2 < \|\mathbf{n}\|_F^2\right) \\ &= P\left(\left\|\sqrt{\tfrac{\rho}{2}}\left[\mathbf{h}_{k_1}\left(x_q - x_{\hat{q}}\right)e^{\,j\theta_k} + \mathbf{h}_{k_2}\left(\tilde{x}_q - \tilde{x}_{\hat{q}}\right)e^{\,j\theta_k}\right] + \mathbf{n}\right\|_F^2 < \|\mathbf{n}\|_F^2\right) \\ &= P\left(\left\|\sqrt{\tfrac{\rho}{2}}[\mathbf{h}_{k_1}d_1 + \mathbf{h}_{k_2}d_2]e^{\,j\theta_k} + \mathbf{n}\right\|_F^2 < \|\mathbf{n}\|_F^2\right), \end{aligned} \tag{A1}$$

where $d_1 = \left(x_q - x_{\hat{q}}\right)$ and $d_2 = \left(\tilde{x}_q - \tilde{x}_{\hat{q}}\right)$.

Let $\mathbf{u} = \sqrt{\frac{\rho}{2}}[\mathbf{h}_{k_1}d_1 + \mathbf{h}_{k_2}d_2]e^{\,j\theta_k}$, the PEP in Equation (A1) can be resolved to

$$\begin{aligned} P\left(\mathbf{x}_{k,q} \to \mathbf{x}_{k,\hat{q}}(\mathbf{H})\right) &= P\left(\|\mathbf{u} + \mathbf{n}\|_F^2 < \|\mathbf{n}\|_F^2\right) \\ &= P\left(\|\mathbf{u}\|_F^2 + 2\Re(\mathbf{n}^{\mathrm{H}}\mathbf{u}) < 0\right) \\ &= P\left(\sum_{i=1}^{N_r}\Re\left(n_i^* u_i\right) > \frac{\sum_{i=1}^{N_r}|u_i|^2}{2}\right), \end{aligned} \tag{A2}$$

where n_i and u_i are the ith element of vectors $\mathbf{n}$ and $\mathbf{u}$, respectively.

From the definition of AWGN in Section 2, n_i follows the distribution given by $n_i \sim CN(0,1)$, where $i \in [1{:}N_r]$. In addition, $n_i^* u_i$ is also a complex Gaussian random variable due to the conditional PEP in Equation (A1) assuming perfect knowledge of all channels. Therefore, $\Re\left(n_i^* u_i\right)$ is a Gaussian random variable with zero mean and variance $\sigma_i^2 = \frac{|u_i|^2}{2}$.

Dividing both sides of the conditional probability by the square root of the variance yields an expression in terms of the definition of the Gaussian $\mathcal{Q}$-function,[33] $\mathcal{Q}(x) = \frac{1}{\pi}\int_0^{\frac{\pi}{2}}\exp\left(\frac{x}{2\sin^2(y)}\right)\mathrm{d}y$, as follows:

$$\begin{aligned} P\left(\mathbf{x}_{k,q} \to \mathbf{x}_{k,\hat{q}}(\mathbf{H})\right) &= P\left(\sum_{i=1}^{N_r}\frac{\Re\left(n_i^* u_i\right)}{\sigma_i} > \frac{1}{2}\sum_{i=1}^{N_r}\frac{|u_i|^2}{\sigma_i}\right) \\ &= \mathcal{Q}\left(\sqrt{\sum_{i=1}^{N_r}\frac{|u_i|^2}{2}}\right) \\ &= \mathcal{Q}\left(\sqrt{\sum_{i=1}^{N_r}v_i}\right), \end{aligned} \tag{A3}$$

where $v_i = \frac{|u_i|^2}{2}$.